Journal of Colloid and Interface Science 358 (2011) 93–101

Contents lists available at ScienceDirect

Journal of Colloid and Interface Science

www.elsevier.com/locate/jcis

Self-assembly behavior and photoluminescence property of bispyrenyl-POSS nanoparticle hybrid

Chu-Hua Lu [a], Chia-Hua Tsai [a], Feng-Chih Chang [a], Kwang-Un Jeong [b], Shiao-Wei Kuo [c,*]

[a] Institute of Applied Chemistry, National Chiao Tung University, Hsin Chu 300, Taiwan
[b] Department of Polymer-Nano Science and Technology, Chonbuk National University, Jeonju 561-756, South Korea
[c] Department of Materials and Optoelectronic Science, Center for Nanoscience and Nanotechnology, National Sun Yat-Sen University, Kaohsiung 804, Taiwan

ARTICLE INFO

Article history:
Received 17 December 2010
Accepted 1 March 2011
Available online 8 March 2011

Keywords:
Polyhedral oligomeric silsesquioxane
Nanocomposites
Photoluminescence
Self-assembly

ABSTRACT

Two flexible ether bonds were designed to connect two pyrene rings on a polyhedral oligomeric silsesquioxane (BPy-POSS) to enrich the fraction of "intrinsic intramolecular pyrene-dimer" on the surface of crystal isobutyl-POSS (iBu-POSS) thin-films. Compared to the monomer emission of 1-pyrenemethanol (Py-OH), the emission spectra of BPy-POSS in dichloromethane show the large proportion of intramolecular and intermolecular excimers due to the formation of pyrenyl dimers or aggregates via the easy rotation of two adjacent ether bonds and the π–π interaction of pyrene rings, respectively. By blending inert iBu-POSS, the fluorescent dimers or aggregates of 5 wt.% and 20 wt.% BPy-POSS are distributed on the surface of iBu-POSS crystal fractal pattern as shown by confocal photoluminescence microscopy. Upon exposure to the vapors of nitrobenzene, the 5 wt.% BPy-POSS blend shows the similar quenching efficiency as 100 wt.% BPy-POSS blends, indicating the better excimer dispersion for vapor permeability of blend thin-films.

1. Introduction

Pyrenyl photoluminescence compounds have been widely used as photosensitive probes in detecting chemical analytes such as nitroaromatic compounds, oxygen, and bimolecules because pyrene has a high quantum yield and a strong affinity with these analytes such as nitroaromatic compounds [1–3]. However, the emission of separate pyrene is in the ultraviolet region (380 nm) incapable of detecting by naked-eye visible sensors. As a result, one strategy for addressing this problem is to use the excimer (a short-lived dimeric or heterodimeric molecule) emissions of pyrene derivatives at 450–500 nm [4]. Many literatures report on photoluminescence sensors of pyrenyl excimers in solution, but not much in their thin fluorescent films [5–7]. To fabricate thin-film photoluminescence sensors for gaseous analytes, spin-coating is one of the most convenient techniques for preparing the sensing layers. In addition to large loss of sample solutions, the spin-coating thin-film of pyrene shows only a weak excimer emission due to a random packing of pyrene rings at a rapid rate of solvent evaporation [8,9]. The intermolecular hydrogen bonding induces the formation of dimer-like excimers by introducing carboxylic acid groups, showing strong visible emission for application of sensing oxygen [10]. However, the analytes with large molecular sizes (e.g. explosive trinitrotoluene, TNT) are difficult to diffuse into the physical network thin-film composed of strong intermolecular interaction such as hydrogen bonds, ionic interaction and so on. This effect of physical network microstructures strongly slows down the response rate of the sensor.

To increase the permeability, the sensing films have to be prepared as thin as possible or the pyrene rings grafted with bulky groups to render a gap for input and output of chemical analytes. Recently, many literatures reported that the bulky organic and inorganic hybrid POSS nanoparticles could effectively reduce the aggregations of photoluminescence units in the active layers of organic molecule and polymer light-emitting diode devices (OLED [11–16] and PLED [17–22]). Furthermore, POSS molecules can be regarded as core–shell colloids with solvated alkyl or aryl shells to disperse insoluble siloxane cores in solution [23–30]. In our previous study [31], we found the specific arrangement of alkyl POSS molecules in a crystal. Like a metal crystal, alkyl POSS has a hexagonal unit cell with the dimensional ratio c/a of 1.06 [31–34]. This value is extremely lower than the expected 1.63 for a hard-sphere-closed-packing mode. Considering the size of alkyl POSS, we concluded that there are small cavities on the surface of an alkyl POSS crystal which are suitable for inserting a POSS molecule, allowing a POSS derivative occupying this position. The wanted

* Corresponding author. Fax: +886 7 5254099.
E-mail address: kuosw@faculty.nsysu.edu.tw (S.-W. Kuo).

0021-9797/$ - see front matter © 2011 Elsevier Inc. All rights reserved.
doi:10.1016/j.jcis.2011.03.003

functional groups can be rich on the surface of an alkyl POSS crystal as long as the functional POSS blends with inert alkyl POSS. In addition, the low dimensional ratio (c/a) of alkyl POSS forms fern-like crystal stripes, composing a thin-film of alkyl POSS crystals. These results imply that we can use a small fraction of functional POSS derivative to cover a large area of POSS crystal. This would be an important characteristic for the design of effective materials in the chemical sensor application. Although, Bai et al. have prepared pyrene-monofunctional isobutyl-POSS (Py-POSS) in the application of the rapid fluorescent detection of TNT [35], we reported the more interesting ether-linked bispyrenyl-monofunctional isobutyl-POSS (BPy-POSS) with the chemical structure shown in Scheme 1a and blended it with inert isobutyl-POSS (iBu-POSS) to fabricate bispyrene-surface-enriched fern-like micropatterns (Scheme 1b) as a chemical sensor for detecting nitroaromatic compounds. With flexible ether bonds, two pyrene rings on a BPy-POSS cage (a butterfly-like structure) would be easier to form intramolecular excimers (close form) which has the stronger excimer emission than Py-POSS. POSS moiety can function as an anchoring group to self-assemble locate itself onto the iBu-POSS crystal templates through POSS–POSS recognition.

2. Experimental

2.1. Materials

1-Pyrenemethanol, 3-chloro-2-chloromethyl-1-propene, trichlorosilane, triethylamine, and the platinum complex (Pt-dvs, 2 wt.% Pt in xylene) were purchased from Aldrich (USA). Prior to use, the solution of the Pt complex was diluted 100-fold with xylene. Toluene and THF were dried by distillation prior to use in the hydrosilylation reactions. Trisilanolisobutyl POSS was purchased from Hybrid Plastics Co. (USA).

2.2. Synthesis of hydride-monofunctional isobutyl-POSS (Si—H iBu-POSS)

Hydride-monofunctional isobutyl-POSS (Si—H iBu-POSS) was synthesized by sol–gel reaction between trisilanolisobutyl POSS® and trichlorosilane ($HSiCl_3$) in anhydrous THF using triethylamine (TEA) to capture HCl in form of an ammonium salt (Scheme 2) [23]. Under Argon atmosphere, Si—H iBu-POSS was obtained by adding a slight excess of $HSiCl_3$ (1.21 ml, 12 mmol) to a 1-l flask containing

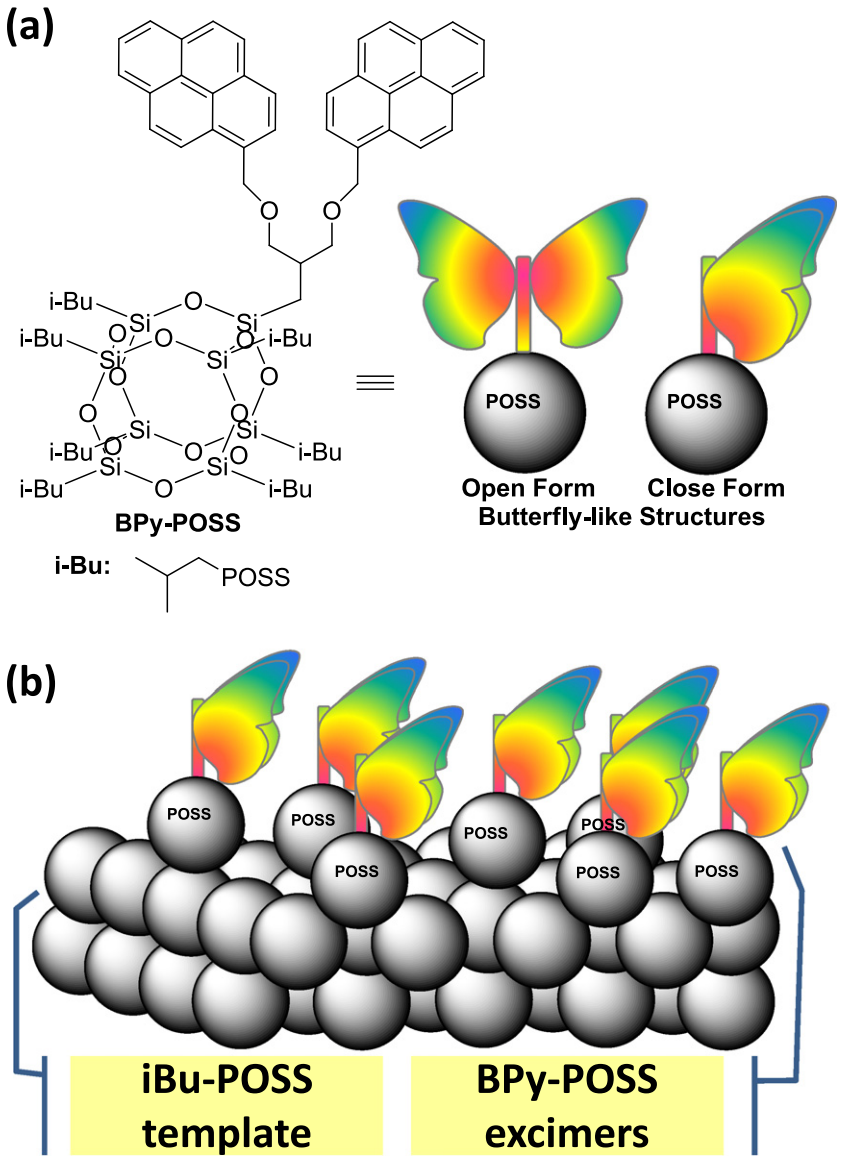

Scheme 1. (a) Open and close forms of BPy-POSS butterfly-like microstructure, (b) Surface enrichment of BPy-POSS on an iBu-POSS crystal.

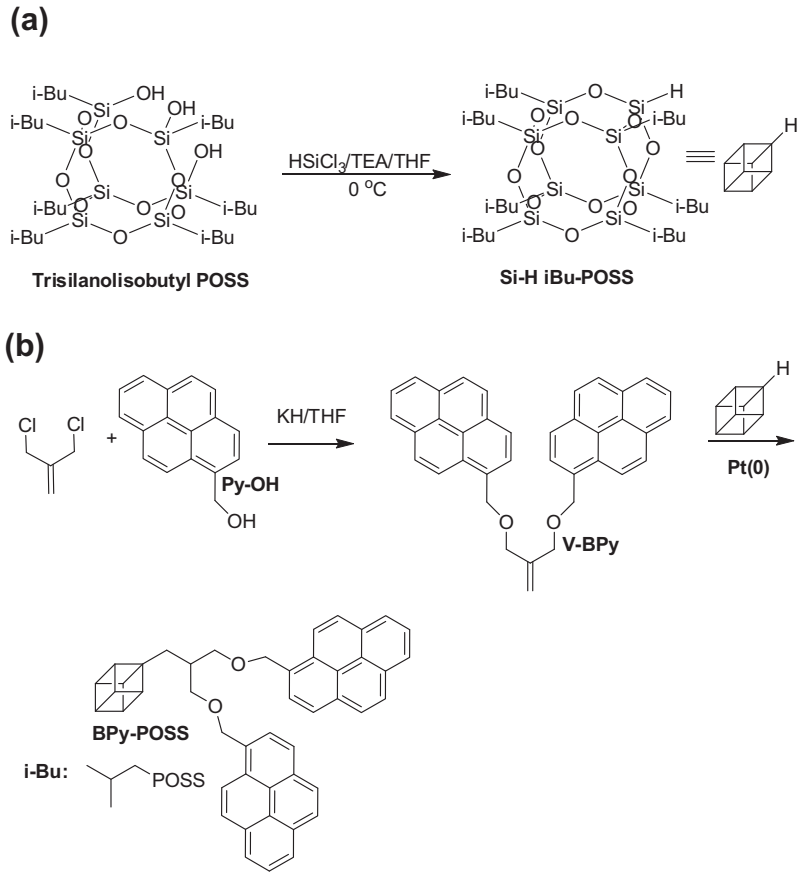

Scheme 2. Synthesis of (a) Si—H iBu-POSS and (b) BPy-POSS.

triSilanolIsobutyl POSS® (7.91 g, 10 mmol), TEA (5.01 ml, 36 mmol) and 800 ml anhydrous THF. The reaction flask was stirred under Argon for 12 h, followed by filtration to remove the byproduct of $HNEt_3Cl$ salts. Si—H iBu-POSS was purified by precipitation from excess ethanol. The 87% yield of Si—H iBu-POSS (11.6 g, 8.7 mmol) was isolated after vacuum drying. Proton nuclear magnetic resonance (^{1}H NMR, in Fig. 1b) (δ, $CDCl_3$): 0.61 (m, 14H, $SiCH_2$), 0.97 (m, 42H, CH_3), 4.11 (s, 1H, SiH).

2.3. Synthesis of vinyl-functional bispyrene (V-BPy)

The vinyl-functional bispyrene (V-BPy) was prepared by etherification reaction of an excess of 1-pyrenemethanol (Py-OH) with methallyl dichloride in anhydrous THF using a strong base of potassium hydride (KH) Scheme 2b). Dry KH (0.43 g, 10 mmol, purification by washing with hexane), methallyl dichloride (0.37 ml, 3.2 mmol) and freshly distilled dry THF (30 ml) were placed in a dry round bottomed flask under Argon atmosphere. At room temperature, Py-OH (2.2 g, 9.5 mmol) was added to the flask with mixture drop by drop. The mixture was stirred at room temperature for 15 min and stirred at 65 °C for 12 h. After cooling to room temperature, the reaction mixture was quenched by water and extracted with dichloromethane. The organic layer then dried over anhydrous $MgSO_4$ and the solvent was removed under vacuum. Purification of the residue by flash column chromatography on silica gel with the same amount of hexane and dichloromethane and yielded 1.32 g of the V-BPy solid (80% yield). Proton nuclear magnetic resonance (^{1}H NMR, in Fig. 1d) (δ, $CDCl_3$): 4.21 (s, 4H, CCH_2O), 5.18 (s, 4H, OCH_2), 5.34 (s, 2H, CH_2CCH_2O), 7.9–8.3 (m, 18H, aromatic).

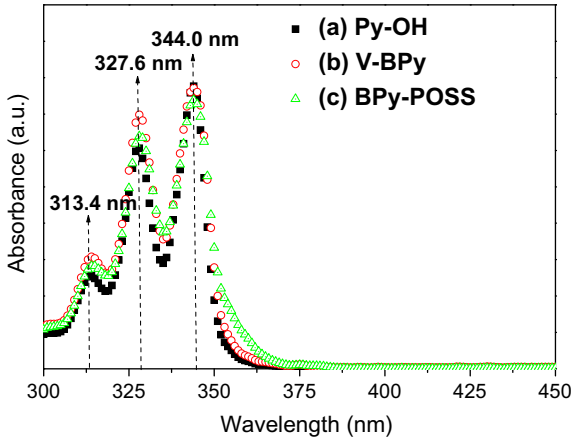

Fig. 1. UV–Vis spectra of dichloromethane solutions (10^{-5} M) of (a) Py-OH, (b) V-BPy, and (c) BPy-POSS.

2.4. Synthesis of bispyrene-monofunctional isobutyl-POSS (BPy-POSS)

The bispyrene-monofunctional isobutyl-POSS (BPy-POSS) was prepared by hydrosilylation reaction of an excess of vinyl-functional bispyrene (V-BPy) with hydride-monofunctional isobutyl-POSS (Si—H iBu-POSS) in anhydrous toluene at 60 °C using a platinum(0) catalyst [Pt(dvs)] (Scheme 2b) [36–39]. A solution of Si—H iBu-POSS (2.5 g, 3 mmol) and V-BPy (15.5 g, 30 mmol) in toluene (60 ml) in a 100-mL Schlenk flask equipped with a reflux condenser and a magnetic stirrer was heated at 60 °C under argon and then Pt(dvs) (0.2 ml, 0.4 μmol) was added via syringe. The reaction, which was monitored by measuring the decrease in intensity of the FT-IR spectra signal at 2134 cm^{-1} for the Si—H bonds, was complete after 24 h. The yellowish, transparent reaction mixture

became clear after removal of the Pt(dvs) catalyst through flash chromatography (neutral Al_2O_3; toluene). The crude product was purified by flash column chromatography on silica gel with hexanes-ethyl acetate (EA:Hexane = 1:8) to yield BPy-POSS (2.5 g, 62%). Proton nuclear magnetic resonance (^{1}H NMR, in Fig. 1e) (δ, $CDCl_3$): 0.61 (s, 16H, $SiCH_2$), 0.95 (s, 42H, CH_3), 1.86 (m, 8H, $SiCH_2CH$), 3.66 (m, 4H, $CHCH_2O$), 5.06 (s, 4H, OCH_2), 7.8–8.21 (m, 18H, aromatic).

2.5. Preparation of iBu-POSS/BPy-POSS blends

BPy-POSS (0.5 mg) and iBu-POSS (9.5 mg) were dissolved in 1 ml solvent to fabricate the 5 wt.% BPy-POSS/iBu-POSS blend solution; BPy-POSS (2 mg) and iBu-POSS (8 mg) were dissolved in 1 ml solvent to make the 20 wt.% BPy-POSS/iBu-POSS blend solution. The blend solutions were stirred for 2 h then the solvent was removed by rotary evaporator. To avoid the residual solvent remained, the samples were put into the vacuum oven for 1 day.

2.6. Characterizations

^{1}H NMR solution spectra were obtained using Varian Unity 300 Hz instrument; *d*-chloroform was the solvent. High-resolution solid-state ^{29}Si NMR spectroscopy experiments were performed at 25 °C using a Bruker DSX-400 spectrometer operating at a resonance frequency of 79.375 MHz. High-resolution solid-state ^{29}Si NMR spectra were acquired with a 90 °C pulse width of 5 μs, a pulse delay time of 2 s, and with the spin rate of 6500 Hz. A Mass spectrum was obtained using a Bruker Daltonics Autoflex III TOF–TOF mass spectrometer. The following voltage parameters were employed: ion source 1, 19.06 kV; ion source 2, 16.61 kV; lens, 8.78 kV; reflector 1, 21.08 kV; reflector 2, 9.73 kV. Thermal analysis was performed with a differential scanning calorimeter from DuPont (DSC-Q20) with a heating rate of 10 °C/min, a cooling rate of 5 °C/min and a temperature range of −90–200 °C. The measurements were made with a 5–10 mg sample in a DSC sample cell; in first scan, the sample was heated from room temperature to 200 °C, after the first heating run, the samples were then cooled to −90 °C and heat again to 200 °C to examine the temperature of glass transition (T_g) and the other transition temperature. After the sample treatment, various concentration of BPy-POSS/iBu-POSS samples were recorded using a TGA-Q50 (TA, USA) over a temperature range of 50–750 °C in a inert atmosphere, at a heating rate of 10 °C/min. UV–Vis spectra were measured using an HP 8453 diode-array spectrophotometer. PL spectrophotometer was used to measure the photoluminescence wavelength of sample film or solution. PL spectra were obtained using a Hitachi F-4500 luminescence spectrometer. The XRD patterns were collected using a D8 Advance Powder X-ray diffractometer (Cu $K\alpha$, 40 kV/40 mA; Bruker, Germany). The scanning rate was 0.6°/min from 2θ = 5–30°. We used the Leica TCS SP5 Confocal Spectral Microscope Imaging System, the excited light source is 100 mW Ar blue laser; the fluorescence microscopy is Leica DMI 6000B CS. One drop of dilute toluene solutions (10 mg/ml of BPy-POSS/iBu-POSS blends solution) was placed onto a glass, and then air-dried at 25 °C. The atomic force microscopy (AFM) employed in this study is a Digital Instruments Veeco Dimension 5000 Scanning Probe Microscope (Veeco Metrology Group). The AFM tapping mode with a 5–10 nm radius silicon tip was used to scan the surface structure, the displacement resolution of AFM is about 0.1 nm. For Transmission Electron Microscopy studies, ultrathin sections of the sample were prepared using a Leica Ulatracut UCU microtome equipped with a diamond knife. Slices of ca. 700 Å thicknesses were cut at room temperature and then the samples were transferred onto the carbon-coated Cu TEM grid. TEM analysis was performed using a Hitachi H-7500 electron microscope operated at 100 kV. The hydrodynamic diameter, Dh, of the BPy-POSS and iBu-POSS solution (in toluene) was measured by dynamic light scattering (DLS). DLS measurements were performed on a Brookheaven 90 plus model equipment (Brookheaven Instruments Corporation, USA) with a He–Ne laser with a power of 35 mW at 632.8 nm. The temperature was controlled at 25 °C, and the measurements were done at an angle of 90°.

3. Results and discussion

3.1. Design of molecule with pyrene-dimer emission in solution

As above mentioned, pyrene-based compounds have two typical emissions: one is the monomer emission of a separate pyrene ring at 380 nm and the other is the excimer emission of a pyrene-dimer or its aggregation at 450–500 nm [4]. Because the latter is visible, we designed the V-BPy to increase the content of the effective excimer emission as shown in Scheme 2b. The chemical structure of the V-BPy is similar to a butterfly, containing two pyrene wings and one vinyl body. The ^{1}H NMR spectrum of the V-BPy was shown in Figure S1 (see the supporting information), indicating that two ether bond were used to connect pyrene and vinyl groups. Comparing to the C—C bond of —CH_2—CH_2—CH_2—, the C—O bond of —CH_2—O—CH_2— without two hydrogen barriers on the oxygen atom is easier to rotate, resulting in the formation of the close form of the butterfly-like microstructure of the V-BPy through intramolecular π–π interaction between two pyrene rings on the V-BPy. This result is proven by UV–Vis and PL spectra. As shown in Fig. 1a, the UV–Vis absorption spectra of the V-BPy in dichloromethane (10^{-5} M) are very similar to that of 1-pyrenemethanol (Py-OH) with the chemical structure shown in Scheme 2, showing the three peaks at 313.4, 327.6, and 344.0 nm corresponding to the vibronic transitions from v = 0 to v' = 0, 1, 2, where v and v' are the quantum vibrational numbers of the ground and excited states, respectively [40]. The solution PL emission spectra (excitation light at 343 nm), however, show something different. In dichloromethane, the Py-OH is dissolved in solution and thus has two sharp monomer emission at 378.8 and 398.0 nm and two shoulder bands at 416.5 and 446.8 nm [35,40,12,41]. In contrast, although the V-BPy is also dissolved in dichloromethane, its PL emission spectrum is composed of a strong excimer emission at 470.7 nm and two weak monomer emissions at 378.8 and 398.0 nm. As reported, the excimer emission at 470.7 nm of pyrene compounds is in accordance with the previous experimental and theoretical works that perfect face-to-face stacking interactions in aromatic π-systems result in an increase in the intensity of the transitions and in turn lead to a red shift of photoluminescence spectra [42–44].

The emission intensity ratio of the excimer band to the monomer band ($I_{470.7}/I_{378.8}$) was calculated to be about 5.2 for the V-BPy. This consequence is reasonable. Based on thermodynamics, the close form of the butterfly-like microstructure is enthalpy-favor due to the intramolecular π–π interaction between two pyrene rings on the V-BPy. However, the easy rotation of two pyrene rings along two C—O bonds possess the advantage of entropy. At temperatures higher than 0 K, the two forms of the butterfly-like microstructures are coexistence. In this study, the enthalpy dominates the conformation of V-BPy and most V-BPy molecules are in the close form of the butterfly-like microstructures in dichloroform at 25 °C. In order to distinguish from the dimer or the aggregation of monopyrene-functional molecules, the excimer emission within a bispyrene molecule such as the V-BPy is called as intramolecular excimer emission in this study. Because the coexistence of two forms of the butterfly-like microstructures is inevitable, we need to define the emission from the aggregation of pyrene groups on

the open forms of the butterfly-like microstructure as intermolecular excimer emission. The definition of intramolecular and intermolecular excimer emission is useful for the study of the V-BPy and the following BPy-POSS in solution or solid phase.

3.2. Design of POSS-based molecule with pyrene-dimer emission

We attached a POSS group to the V-BPy as an anchor to fix the bispyrene fluorescent onto the surface of the additional POSS crystal. It is well-known that the hydrosilylation addition between silane (RSi—H) and vinyl (CH_2 = CHR′) groups has conversions up to 100% [3]. But the silicon can be added onto two carbons resulting in two isomeric products: α-(RSi—CHR′(CH_3)) and β-(RSi—CH_2—CH_2R′) [38]. In this study, the hydrosilylation addition between Si—H iBu-POSS and V-BPy produces the BPy-POSS with the linkage of β-(RSi—CH_2—CH_2R′) (see ^{1}H NMR and ^{29}Si NMR spectra in the supporting information). In view of the chemical structure, the formation of the β-linkage with less steric hindrance could be due to two bulky reactants of V-BPy and Si—H iBu-POSS [23]. In addition, the MALDI-TOF mass spectrum of BPy-POSS shows a single peak at 1441.40 g/mol for its Ag^+-complex (also see Figure S2b in the supporting information) [16,40,12]. Indeed, the mass spectrum is more powerful than NMR spectra to support the new compound of BPy-POSS because the silane and the vinyl-functional groups are too small in comparison to the bulky body of the Si—H iBu-POSS and the V-BPy.

The UV–Vis absorbane and PL emission spectra of the BPy-POSS in dichloromethane (10^{-5} M) are also observed in Fig. 1. The BPy-POSS shows the same absorbance bands (313.4, 327.6, and 344.0 nm) as Py-OH and V-BPy [12]. However, the PL emission spectrum (excitation light at 343 nm) of the BPy-POSS is different, having three monomer emissions at 385.5, 404.2, and 426.8 nm, one intramolecular excimer emission at 470.8 nm. Compared to the excimer emission of the V-BPy, the BPy-POSS is broader and in detail, another weak excimer emission at 498.3 nm overlaps with the intramolecular excimer emission. In addition, the emission intensity ratio of the excimer band to the monomer band ($I_{470.7}/I_{385.5}$) was calculated to be about 0.63 for the BPy-POSS which is much lower than 5.2 for the V-BPy. These results imply that the BPy-POSS could be in form of aggregation rather than an individual molecule so as to produce the stronger monomer emission and the "intermolecular excimer emission" at 498.3 nm. The following dynamic light scattering analysis of the BPy-POSS can support this concept as shown in Fig. 2b. According to the size of the individual BPy-POSS (see the calculation and Figure S3 in the supporting information), the hydrodynamic diameter of 22.4 nm is large enough to confirm the aggregation of the BPy-POSS in dichloromethane. The chemical structure of the BPy-POSS is composed of two parts: one is bispyrene and the other is POSS. Compared to the hydrodynamic diameter of 3.72 nm for inert isobutyl-POSS (iBu-POSS) in Fig. 2a, we supposed that the intermolecular π–π interaction of pyrene rings of BPy-POSS molecules plays a significant role in the aggregation of the BPy-POSS in the dichloromethane as shown in Scheme 3.

In dichloromethane, the PL emission spectra tell us the conformation of the Py-OH, V-BPy, and BPy-POSS. The solid-state PL emission spectrum is also important to reveal their conformation without solvent. This would be more significant for us. The solid-state photoluminescent spectra (excitation light at 343 nm) of the Py-OH, V-BPy, and BPy-POSS prepared by spin-coating (500 rpm) of dichloromethane solutions (10 mg/mL) on a 2 cm × 2 cm quartzes are shown in Fig. 3.

The Py-OH is a typical small molecule and crystalized when the solvent is evaporated. Thus, the solid-state PL emission spectrum of the Py-OH shows the excimer emission of the Py-OH crystal where the pyrene group is adjacent to one another. The solid-state

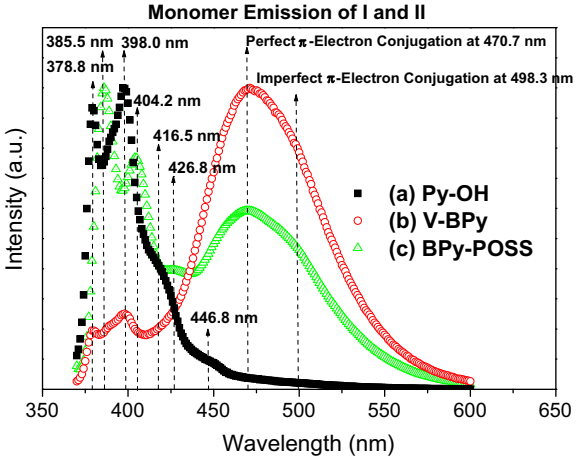

Fig. 2. Normalized emission and excitation spectra of dichloromethane.

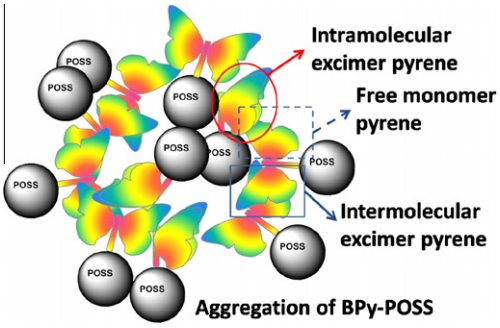

Scheme 3. BPy-POSS aggregation in solution photoluminescence spectra.

PL emission spectra of the V-BPy and the BPy-POSS have the similar excimer emissions as the Py-OH. Compared to the results of solution PL spectra in Fig. 1b, they in dichloromethane show something different, especially having the low fraction of monomer emission intensities in the solid-state PL spectra. For the BPy-POSS, we supposed that the aggregation of the BPy-POSS should be dissolved in solution and rearranged in the BPy-POSS solid while the dichloromethane evaporates. As we discussed above, the thermodynamics induces the coexistence of intramolecular and intermolecular π–π interaction of the V-BPy in dichloromethane. The

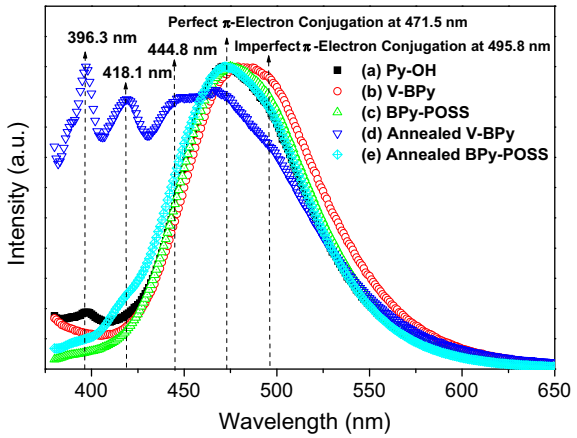

Fig. 3. Normalized emission and excitation spectra of thin-film samples of (a) Py-OH, (b) V-BPy, (c) BPy-POSS, (d) thermal annealed V-BPy, and (e) thermal annealed BPy-POSS.

spin coating is a kinetically controlled procedure because most solution is thrown out by the centrifugal force and the residue solvent is dried more quickly than usual. After the heat treatment at 150 °C for 1 h under vacuum, the monomer emissions of the annealed V-BPy occur at 396.3, 418.1, and 444.8 nm. In comparison, the excimer emission of the annealed BPy-POSS is similar to that before the heat treatment. From the DSC thermogram of the BPy-POSS in Fig. 4a (see the discussion), we inferred that with phase separation, the POSS domains of the BPy-POSS could promote the formation of the close form of the bispyrene via the intramolecular π–π interaction. To compare the solution and the solid-state PL spectra of the BPy-POSS, we can find that the BPy-POSS in solid-state tends to form the thermally stable close form of the butterfly-like microstructure through intramolecular π–π interaction.

3.3. Immiscible blends of iBu-POSS and BPy-POSS

For most studies, POSS derivatives are used to investigate their bulk microstructures and unique properties [36]. In our previous study [31], we found that alkyl POSS molecules tend to form a thin-film composed of fern-like striped crystals. More interestingly, we can put POSS derivatives on the surface of alky POSS crystals through the POSS-POSS stacking. Thus, the POSS–POSS stacking would be an alternative method to achieve the surface enrichment of specific functional groups as long as this functional group is grafted onto a POSS, mixed with alkyl POSS, and then dried a drop of solution on a substrate. In this case, the inert isobutyl-POSS (iBu-POSS) is used to blend with BPy-POSS. To our design, we hope that BPy-POSS is immiscible with iBu-POSS and BPy-POSS aggregation or molecules can be dispersed on the surface of iBu-POSS crystals. Similar to polymer blends, we managed to study the immiscibility of blends between iBu-POSS and BPy-POSS by DSC thermograms. In the second heat process, the iBu-POSS has a melting point at 56.0 °C and the V-BPy has a glass transition temperature at 14.6 °C in Fig. 4a [36]. Herein, the glass transition of the V-BPy indicates that the dissymmetric V-BPy at low temperatures is a glasslike substance but not a crystal although V-BPy is a small molecule rather than a macromolecule. The BPy-POSS possess one glass transition temperature at 14.2 °C, one recrystallization temperature at 62.7 °C, and one melting temperature at 127.7 °C. Comparing to iBu-POSS and V-BPy, we suggested that the BPy-POSS is more like to a block copolymer with distinct phases and then has a glass transition for the bispyrene domain and a melting transition for the POSS domain. Because the bulky bispyrene is attached onto a POSS, the BPy-POSS need more energy to stacking POSS molecules in form of a crystal resulting in the higher melting temperature of the POSS domain. Two phases of the BPy-POSS can be inferred from its TEM image (see Figure S4 in the supporting information).

For a homogeneous material, we cannot observe any difference in a TEM image. In contrast, the needle-like microstructures represent the aggregation of the BPy-POSS in the solid-state and this aggregation is induced by the phase separation of bispyrene and POSS domains. In fact, the morphology of the BPy-POSS in the solid-state is not very important for the immiscible blend with iBu-POSS. Instead, we are more interested in the dispersion of the BPy-POSS on the surface of iBu-POSS crystals. Fig. 4b shows the DSC thermograms of the iBu-POSS blends with the different weight fraction of BPy-POSS. For 5 and 20 wt.% BPy-POSS, the baselines slightly descend at 23.7 °C due to the presence of bispyrene domains. However, these results are not clear to prove the immiscibility between iBu-POSS and BPy-POSS. To increase the content of BPy-POSS up to 50 wt.%, the glass transition and the melting temperatures of the BPy-POSS are observed at 23.7 and 122.0 °C besides the melting temperature of iBu-POSS occurs at 53.6 °C. Three domains indicate the phase separation of the immiscible blend between iBu-POSS and BPy-POSS.

3.4. Surface enrichment of pyrene-dimer fluorescent on POSS crystals

In view of the device to detect the dynamic contacting angle of one drop on a specific substrate, we discovered the method of the preparation of an iBu-POSS crystalline thin-film. As depicted in Scheme 4, a solution of iBu-POSS (10 mg/ml in toluene) is spread on a substrate through a droper and subsequently, excess solution is withdrawn by the same droper.

This procedure is called the advancing and receding solution process. The fern-like striped crystals of iBu-POSS occur along the receding border between the solution and the substrate; the thin-film of iBu-POSS is constructed by these stripe crystals with lateral dimensions on the order of a few micrometers and thickness of a few hundred nanometers [31,45]. As shown in Fig. 5, the stripes of the iBu-POSS blend containing 5 wt.% BPy-POSS are observed by the AFM analysis, for example a typical one of 2.93 μm in width and 198.30 nm in height [31]. Similar microstructure of the iBu-POSS blends containing 20 wt.% BPy-POSS is also detected, such as one stripe of 3.75 μm in width and 140.87 nm in height.

Interestingly, we found that the surface of the latter is rougher than the former. By XRD analyses, Fig. 6c shows the similar amorphous halo to the pure BPy-POSS at 2θ of 15–25° for the iBu-POSS blend containing 20 wt.% BPy-POSS, indicating that the dispersion

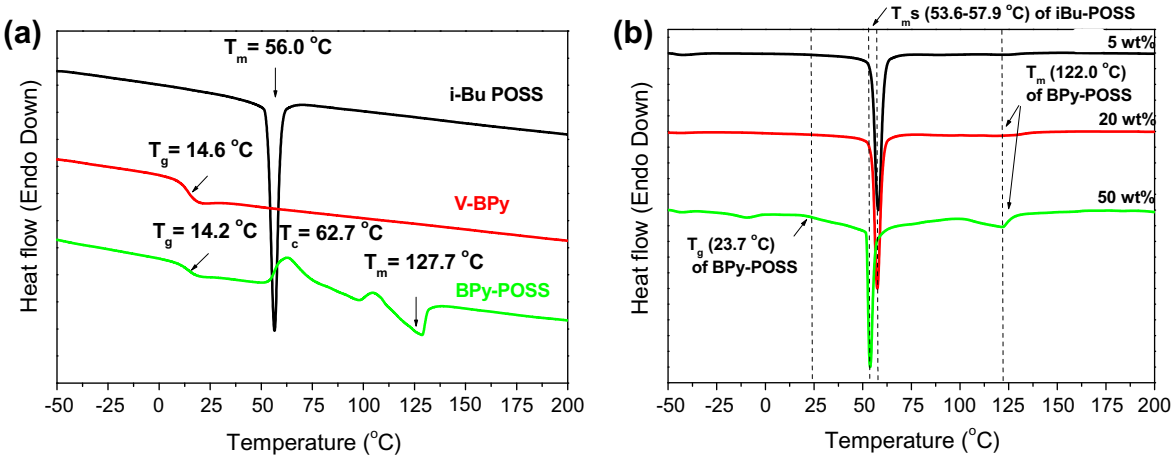

Fig. 4. DSC thermograms of (a) iBu-POSS, V-BPy, BPy-POSS and (b) the iBu-POSS blends with different weight fractions of BPy-POSS.

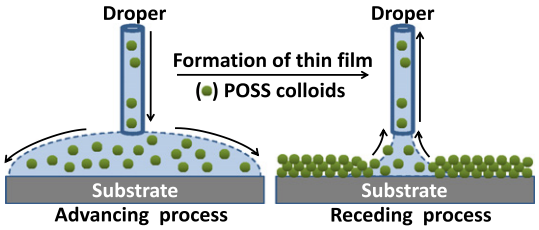

Scheme 4. Formation of alkyl POSS crystal stripes though advancing and receding solution process.

of the aggregation of the BPy-POSS on the surface of the iBu-POSS crystals stripes results in the rough surface as shown in Fig. 5b. To compare the relatively smooth surface of the iBu-POSS containing 5 wt.% BPy-POSS as shown in Fig. 5a, 20 wt.% BPy-POSS seems too many to cover a thin layer on the surface of the iBu-POSS crystal stripes. In other words, the iBu-POSS blend containing 5 wt.% BPy-POSS would has more economic efficiency to be a chemical sensor to detect nitrobenzene in this study.

The confocal photoluminescent microscopy (CPLM) is the more powerful analytic method to prove the surface enrichment of the BPy-POSS on the surface of the iBu-POSS crystal stripes because only BPy-POSS has a fluorescent bispyrene group. Herein, the CPLM provides three images: optical microscopy (OM), photoluminescent microscopy (PLM), and their superposition image (OM-PLM). For pure iBu-POSS, the fern-like crystal stripes can be observed by the OM image as shown in Fig. 7a. Blending with 5 and 20 wt.% BPy-POSS, the similar microstructures are visible by the PLM image as shown in Fig. 7b. Compared to pure BPy-POSS, the OM and PLM images do not show any regular pattern. This information reveals that the BPy-POSS is indeed dispersed on the surface of the iBu-POSS crystal stripes resulting in the thin-film of the iBu-POSS crystals containing BPy-POSS on their surface.

3.5. Chemosensor application using surface enrichment of BPy-POSS

A simple apparatus is designed to measure the fluorescence quenching of pyrene excimer emission with nitrobenzene in a close system [35]. The iBu-POSS blends with 5, 20, 100 wt.% BPy-POSS are coated on the 2 cm × 2 cm quartz by the above mentioned method and then are placed in a 10 cm × 10 cm × 10 cm plastic airtight container with two 2 cm × 2 cm quartz windows in the light pathway and a glass holder. After 0.5 ml nitrobenzene was injected in the glass holder through syringe, the spectrometer starts to in situ detect PL intensities at 470 nm under the excited wavelength of 343 nm. As shown in Fig. 8, the PL decays of 56%, 78%, 58% are observed for the excimer emission of the iBu-POSS blends containing 5, 20 and 100 wt.% BPy-POSS after exposing to a nitrobenzene atmosphere for 10 min, indicating the nitrobenzene liquid (b.p. ~211 °C) evaporates and permeates in the cover layer of BPy-POSS. For convenience of discussion, the quenching efficiency was calculated using the following equation:

$$\eta = \frac{I_0 - I}{I_0} \times 100\% \quad (1)$$

As shown in Fig. 9, 1-min exposure of the iBu-POSS blends with 5, 20, and 100 wt.% BPy-POSS to nitrobenzene vapor causes nearly 15, 20, and 30% quenching of the eximer emission at 470 nm. Herein, the 15% decay of the PL emission within 1 min for the iBu-POSS

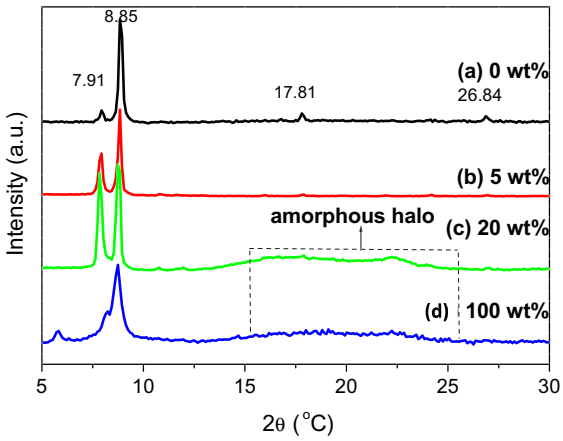

Fig. 6. Solid-state XRD analyses of iBu-POSS blends with (a) 0, (b) 5, (c) 20, and (d) 100 wt.% BPy-POSS on a silicon wafer.

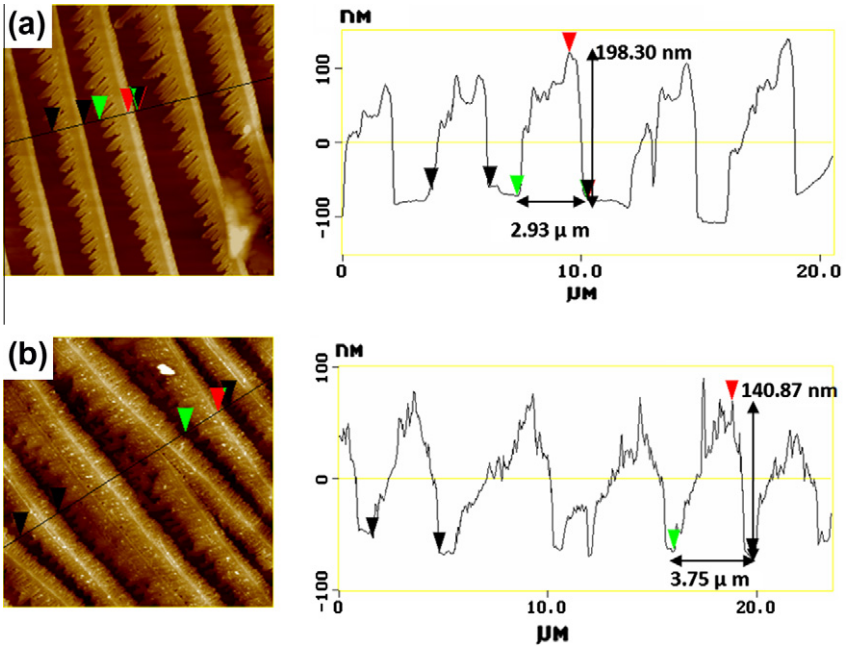

Fig. 5. AFM 2D images and sectional analyses of iBu-POSS blends with (a) 5 and (b) 20 wt.% BPy-POSS in the scanning scale of 20 × 20 μm².

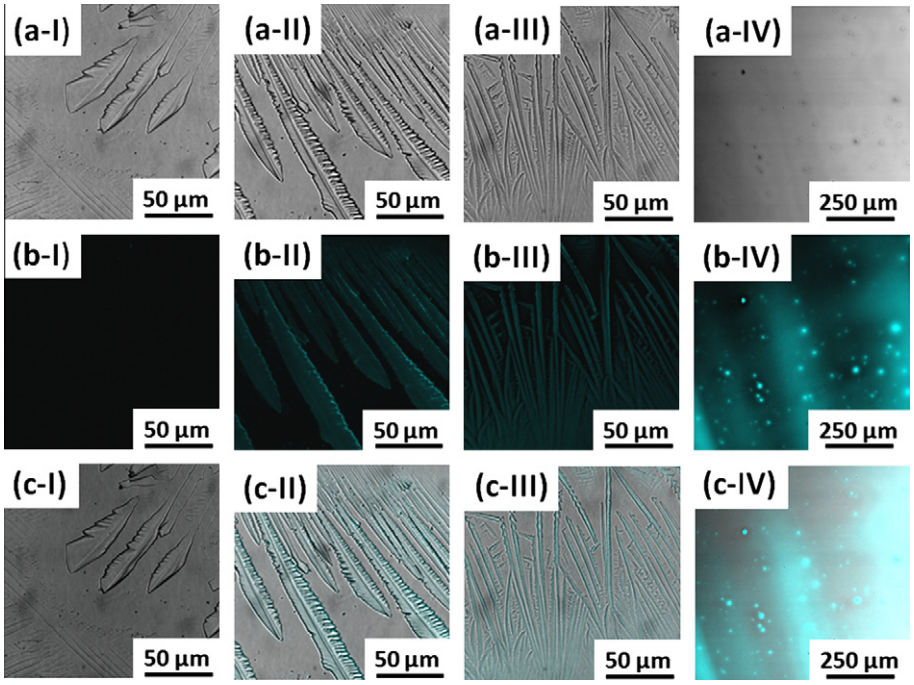

Fig. 7. (a) OM images, (b) PLM images, and (c) OM-PL superimposed images of iBu-POSS blends with (I) 0, (II) 5, (III) 20, (IV) 100 wt.% BPy-POSS.

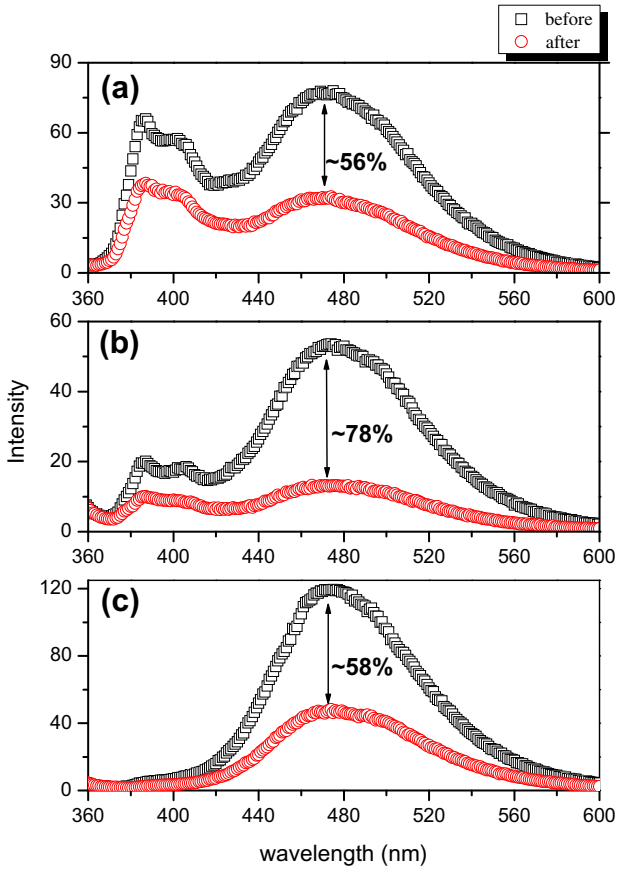

Fig. 8. Solid-state PL spectra of iBu-POSS blends with (a) 5, (b) 20, and (c) 100 wt.% BPy-POSS before and after exposure to nitrobenzene vapor for 10 min.

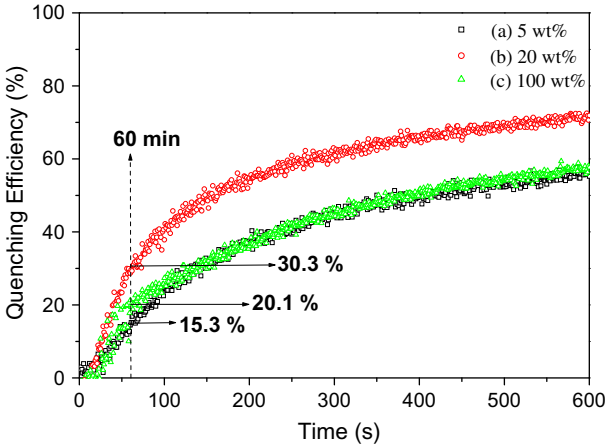

Fig. 9. Time-dependant quenching efficiency of iBu-POSS blends with (a) 5, (b) 20, (c) 100 wt.% BPy-POSS on exposure to nitrobenzene vapor.

blend containing 5 wt.% BPy-POSS is clear and quick enough to detect the leakage of nitrobenzene vapor. Based on the above discussion, the iBu-POSS blend containing 5 wt.% BPy-POSS would be the better composition for the chemosensor to cover the thin layer of fluorescent BPy-POSS on the surface of the iBu-POSS crystal film.

4. Conclusions

A novel bispyrenyl-functional polyhedral oligomeric silsequioxanes (BPy-POSS) is designed and synthesized for detecting nitrobenzene vapor. Like organic small molecules, iBu-POSS is crystal (T_m of 56.0 °C) but the dissymmetric BPy-POSS with two pyrene rings is semicrystal (T_g of 14.2 °C, T_c of 62.7 °C, and T_m of 127.7 °C). Most monofunctional pyrene compounds can be well dissolved in solvent, resulting in invisible monomer emission. With flexible ether bonds, two pyrene rings of BPy-POSS tends to form the intramolecular dimer (π–π stacking), which is active and visible for detecting nitrobenzene. Besides, the POSS moiety could help BPy-POSS well-disperse on the surface of iBu-POSS crystals after

solvent evaporation of BPy-POSS/iBu-POSS mixtures. Mixing with 5 wt.% BPy-POSS in iBu-POSS, the blend has the bright fern-like fractal pattern under UV light excitation (343 nm), indicating the distribution of BPy-POSS on the surface of iBu-POSS crystal patterns. Upon exposure to nitrobenzene vapor, the similar results of the blends with 5 wt.% and 100 wt.% BPy-POSS prove that BPy-POSS is a useful and economical nanomaterial for chemosensor application.

Acknowledgments

This study was supported financially by the National Science Council, Taiwan, Republic of China, under contracts NSC97-2221-E-110-013-MY3, and NSC 98-2120-M-009-001.

Appendix A. Supplementary material

Supplementary data associated with this article can be found, in the online version, at doi:10.1016/j.jcis.2011.03.003.

References

[1] W. Xu, R. Schmidt, M. Whaley, J.N. Demas, B.A. DeGraff, E.K. Karikari, B.A. Famer, Anal. Chem. 67 (1995) 3172.
[2] S.J. Zhang, F.T. Lü, L.N. Gao, L.P. Ding, Y. Fang, Langmuir 23 (2007) 1584.
[3] X.Y. Pan, Q.J. Cai, C.M. Li, Q. Zhang, P.M.B. Chan, Nanotechnology 20 (2009) 305601.
[4] J.B. Birks, Rep. Prog. Phys. 38 (1975) 903.
[5] S.K. Kim, J.H. Bok, R.A. Bartsch, J.Y. Lee, J.S. Kim, Org. Lett. 7 (2005) 4839.
[6] B.N. Boden, K.J. Jardine, A.C.W. Leung, M.J. MacLachlan, Org. Lett. 8 (2006) 1855.
[7] Y. Shiraishi, Y. Tokitoh, G. Nishimura, T. Hirai, J. Phys. Chem. B 111 (2007) 5090.
[8] H. Bai, C. Li, G.Q. Shi, Sens. Actuators, B 130 (2008) 777.
[9] Y. Fujiwara, Y. Amao, Sens. Actuators, B 89 (2003) 187.
[10] Y. Fujiwara, I. Okura, T. Miyashita, Y. Amao, Anal. Chim. Acta 471 (2002) 25.
[11] H.J. Cho, D.H. Hwang, J.I. Lee, Y.K. Jung, J.H. Park, J. Lee, S.K. Lee, H.K. Shim, Chem. Mater. 18 (2006) 3780.
[12] I. Imae, Y. Kawakami, J. Mater. Chem. 15 (2005) 4581.
[13] Y. Xiao, L. Liu, C. He, W.S. Chin, T. Lin, K.Y. Mya, J. Huang, X. Lu, J. Mater. Chem. 16 (2006) 829.
[14] P. Andre, G. Cheng, A. Ruseckas, T.V. Mourik, H. Fruchtl, J.A. Crayston, R.E. Morris, D. Cole-Hamilton, I.D.W. Samuel, J. Phys. Chem. B 112 (2008) 16382.
[15] J.D. Froehlich, R. Young, T. Nakamura, Y. Ohmori, S. Li, A. Mochizuki, Chem. Mater. 19 (2007) 4991.
[16] C.C. Cheng, C.H. Chien, Y.C. Yen, Y.S. Ye, F.H. Ko, C.H. Lin, F.C. Chang, Acta Mater. 57 (2009) 1938.
[17] K. Zhang, Z. Chen, C. Yang, X. Zhang, Y. Tao, L. Duan, L. Chen, L. Zhu, J. Qin, Y. Cao, J. Mater. Chem. 17 (2007) 3451.
[18] W. Zhao, T. Cao, J.M. White, Adv. Funct. Mater. 14 (2004) 783.
[19] S. Xiao, M. Nguyen, X. Gong, Y. Cao, H. Wu, D. Moses, A.J. Heeger, Adv. Funct. Mater. 13 (2003) 25.
[20] J. Miyake, Y. Chujo, Macromol. Rapid Commun. 29 (2008) 86.
[21] J.M. Kang, H.J. Cho, J. Lee, J.I. Lee, S.K. Lee, N.S. Cho, D.H. Hwang, H.K. Shim, Macromolecules 39 (2006) 4999.
[22] J. Miyake, Y. Chujo, J. Polym. Sci., Polym. Chem. 46 (2008) 6035.
[23] R.H. Baney, M. Itoh, A. Sakakibara, T. Suzuki, Chem. Rev. 95 (1995) 1409.
[24] K.J. Shea, D.A. Loy, Acc. Chem. Res. 34 (2001) 707.
[25] H. Xu, S.W. Kuo, J.S. Lee, F.C. Chang, Macromolecules 35 (2002) 8878.
[26] Y.L. Liu, Y.H. Wu, R.J. Jeng, S.A. Dai, J. Colloid Interface Sci. 336 (2009) 198.
[27] S.W. Kuo, H.F. Lee, W.J. Huang, K.U. Jeong, F.C. Chang, Macromolecules 42 (2009) 1619.
[28] S.W. Kuo, Y.C. Wu, C.H. Lu, F.C. Chang, J. Polym. Sci. Polym. Phys. 47 (2009) 811.
[29] Y.J. Yen, S.W. Kuo, C.F. Huang, J.K. Chen, F.C. Chang, J. Phys. Chem. B 112 (2008) 10821.
[30] C.F. Huang, S.W. Kuo, F.J. Lin, W.J. Huang, C.F. Wang, W.Y. Chen, F.C. Chang, Macromolecules 39 (2006) 300.
[31] C.H. Lu, S.W. Kuo, C.F. Huang, F.C. Chang, J. Phys. Chem. C 113 (2009) 3517.
[32] A.J. Waddon, E.B. Coughlin, Chem. Mater. 15 (2003) 4555.
[33] L. Cui, J.P. Collet, G. Xu, L. Zhu, Chem. Mater. 18 (2006) 3503.
[34] J. Miao, L. Cui, H.P. Lau, P.T. Mather, L. Zhu, Macromolecules 40 (2007) 5460.
[35] H. Bai, C. Li, G. Shi, Chem. Phys. Chem. 9 (2008) 1908.
[36] Y.C. Sheen, C.H. Lu, C.F. Huang, S.W. Kuo, F.C. Chang, Polymer 49 (2008) 4017.
[37] H.C. Lin, S.W. Kuo, C.F. Huang, F.C. Chang, Macromol. Rapid Commun. 27 (2006) 537.
[38] S.W. Kuo, H.C. Lin, W.J. Huang, C.F. Huang, F.C. Chang, J. Polym. Sci. Part B: Polym. Phys. 44 (2006) 673.
[39] K.W. Huang, L.W. Tsai, S.W. Kuo, Polymer 50 (2009) 4876.
[40] I. Imae, Y. Kawakami, Y. Ooyama, Y. Harima, Macromol. Symp. 50 (2007) 249.
[41] F.M. Winnik, Chem. Rev. 93 (1993) 587.
[42] Y.H. Kim, D.K. Yoon, E.H. Lee, Y.K. Ko, H.T. Jung, J. Phys. Chem. B 110 (2006) 20836.
[43] V. Zucolotto, A.D. Faccto, F.R. Santos, C.R. Mendonca, F.E.G. Guimaras, O.N. Oliveira, J. Phys. Chem. B 109 (2005) 7063.
[44] K. Ye, J. Wang, H. Sun, Y. Liu, Z. Mu, F. Li, S. Jiang, J. Zhang, H. Zhang, Y. Wang, C.M. Che, J. Phys. Chem. B 109 (2005) 8008.
[45] L. Larsson, Ark. Kemi 16 (1960) 209.